DOI: https://doi.org/10.57233/ijsgs.v11i3.949 ISSNp: 2488-9229; ISSNe: 3027-1118

IJSGS FUGUSAU VOL.11(3) WEBSITE: https://fugus-ijsgs.com.ng

INTERNATIONAL JOURNAL OF SCIENCE FOR GLOBAL SUSTAINABILITY
(A PUBLICATION OF FACULTY OF SCIENCE, FEDERAL UNIVERSITY GUSAU, NIGERIA)

# Judd-Offelt Analysis of Sm/Dy Codoped Borate-Based Glasses Co-embedded with Gold and Silver Nanoparticles.

**I. Abdullahi[a*], A.B. Isah[a], Y. Usman[a], M. Bello[a] and Y.A., Yamusa[b]**

[a]Department of Physics Federal University Gusau, Zamfara State Nigeria
[b]Department of Physics Ahmadu Bello University, Zaria, Nigeria

***Corresponding Author's Email:** Ibrahimabdullahi@fugusau.edu.ng.

**Received on:** August, 2025 **Revised and Accepted on:** September, 2025 **Published on:** October, 2025

***ABSTRACT***

Metallic nanoparticles through their localized surface plasmon resonance plays a vital role in enhancing the optical absorption and emission of rare earth ions doped glasses aimed at optics/photonic applications. In this work, a series of borate based glasses was synthesized and co-embedded with gold and silver nanoparticles through melt-quenching technique. Judd-Ofelt analysis was done to determine the absorption and emission traits. The Uv-Vis-NIr absorption measurement revealed eleven $^6H_{15/2}$ to manifold absorption bands. While the addition of 0.03 mol% of AgNPs saw the reduction in the absorption intensity as revealed by S2 glass sample, the addition of 0.1 mol% nanoparticles saw the enhancement of the absorbance attaining the highest value as proved by S3 glass sample. Bandgap energies for the developed glasses were determined using Tauc's plot with S4 producing the highest value of 2.3 eV. Furthermore, the oscillator strength of transition $^6F_{5/2}$ was found to be decreased from 0.374 to 0.178 $\times 10^{-6}$ while that of $^6F_{7/2}$ increased from 0.589 to 0.594$\times 10^{-6}$ with the introduction of the nanoparticles co-embedder. Judd-Ofelt intensity parameters $\Omega_2$, $\Omega_4$ and $\Omega_6$ were derived from the oscillator strengths and the magnitude of $\Omega_2$ corresponding to S0 decreased down to 0.81 $\times 10^{-20}$ cm$^2$ from 1.15$\times 10^{-20}$ cm$^2$ which is further reduced to 0.58$\times 10^{-20}$ cm$^2$ with the co-embedding activity. Perhaps, structural re-adjustments within the glass network is responsible for the observed fluctuations. Conclusively, due to the achieved striking absorption and emission cross-sections, we suggests that the present glass-REions-metallic nanoparticles combination may be useful for laser and white light emitting diodes applications.

**Keywords:** Judd-Ofelt, silver nanoparticles, co-embedment, rare earth ions, glasses

## 1.0 INTRODUCTION

Rare-earth (RE)-doped glasses proved to be promising in the development of robust and advanced optics/photonic materials such as microelectronics, LEDs, lasers, and fluorescent materials (Basha et al., 2024; Boudchicha et al., 2023; Hossain et al., 2022; Muhammad et al., 2022; Rivera et al., 2023). The electrons in their partially filled 4f orbitals are shielded by the outer 5s and 5p orbitals, making the corresponding energy levels independent of the surrounding environment t. This ensures a narrow and well-defined energy levels, which produce sharp emission lines in the event of electronic transitions (Weber, 1990). Thus, they can emit light in precisely defined colours, including ultraviolet (UV), visible, and near-infrared (NIR). This makes them useful for many scientific applications, including solid-state lasers, optical amplifiers, sensors, fibre optics, and lighting devices (Ahmad et al., 2020). However, the intensity of emission from RE ions was found to depend heavily on the chosen host matrix (Singh et al., 2025).

The dominant RE ions hosts are either crystalline or glasses, compared with crystalline hosts, glasses are easier to process, more flexible in their composition, and cheaper (Abdullahi, Hashim, Ghoshal, & Ahmad, 2020). They can incorporate multiple dopants, which makes them excellent candidates for co-doped systems where the effects of RE ions can be used together to enhance the overall performance. However, the fact that 4f-4f transitions are parity-forbidden means they are less efficient at absorbing light. This has led to ongoing research into changing the structure of glass hosts and using sensitizers, like nanoparticles, to make the light brighter (Abdullahi, Hashim, Ghoshal, & Sa'ad, 2020).

There are different RE activators, and samarium ($Sm^{3+}$) and dysprosium ($Dy^{3+}$) have attracted a lot of attention because of their complementary visible emission bands (Ghosh et al., 2022). $Sm^{3+}$ ions show strong orange-red light, mostly from the $^4G_{5/2} \rightarrow {}^6H_J$ transitions (J = 5/2, 7/2, 9/2, 11/2). This is useful for divers applications like display technologies, red phosphors and lasers that operate in the orange part of the spectrum (Abdullahi et al., 2019; Li et al., 2022). The orange ($^4G_{5/2} \rightarrow {}^6H_{7/2}$) and red ($^4G_{5/2} \rightarrow {}^6H_{9/2}$) lines react very strongly to changes in the structure around them, this makes $Sm^{3+}$ a useful tool for measuring local symmetry and the strength of bonds (Ghosh et al., 2022).

DOI: https://doi.org/10.57233/ijsgs.v11i3.949 ISSNp: 2488-9229; ISSNe: 3027-1118



$Dy^{3+}$ ions, on the other hand, produce two strong bands of light in the visible spectrum: a blue line at $^4F_{9/2} \rightarrow {}^6H_{15/2}$ (~480 nm) and a yellow line at $^4F_{9/2} \rightarrow {}^6H_{13/2}$ (~575 nm). The yellow band is very sensitive to changes in the ligand field, which shows asymmetry in the host glass (Abdullahi, Hashim, Ghoshal, & Ahmad, 2020). By changing how much blue and yellow light is produced, $Dy^{3+}$-doped glasses can produce a white light, which makes them useful for solid-state lighting and phosphor-converted LEDs. When $Sm^{3+}$ and $Dy^{3+}$ are combined, energy can be transferred between the $Dy^{3+}$ (donor) and the $Sm^{3+}$ (acceptor) ions. This leads to a change in the amount of light given off in the blue, yellow, and orange-red parts of the spectrum (Liang et al., 2023). This special method of doping allows you to adjust the colour and control the brightness, which makes the white light better than it would be with just one type of doping. However, there are not many studies that look at $Sm^{3+}/Dy^{3+}$ codoped borate glasses in detail, especially when it comes to spectroscopic modelling.

The host matrix is very important in determining the performance of rare-earth ions when it comes to spectroscopy. Borate glasses, which are made from $B_2O_3$, are some of the most useful hosts because they can form well, they are very clear in the UV-visible range, they have low phonon energies, and they can contain high concentrations of rare-earth dopants without severe clustering or concentration quenching (Ahmad et al., 2020; Nagaraj et al., 2017). These properties make borate glasses better than silicates and phosphates, which often have higher phonon energies, and fluoride glasses, which significantly lacks chemical stability (Phi et al., 2019).

Borate glasses are made up of triangular $BO_3$ and tetrahedral $BO_4$ units. the proportion of these units can be modified by adding network modifiers, such as alkali ($Li_2O$, $Na_2O$) or alkaline earth oxides (SrO, ZnO). These convert $BO_3$ units into $BO_4$ tetrahedra, reducing non-bridging oxygens and making the network more rigid (Zhang et al., 2023). This structural flexibility directly affects the local environment of RE ions, which then changes how likely they are to emit a photon and how efficiently they do so. For example, $Dy^{3+}$ in Li–Sr–Zn–borate glasses shows strong yellow colouration because of the uneven way the atoms are arranged. This makes the $^4F_{9/2} \rightarrow {}^6H_{13/2}$ transition stronger (Ahmad et al., 2020; M.C. et al., 2012). In addition, borate glasses are practical for large-scale photonic devices because they have good thermal stability, low melting temperatures, and can be easily manufactured. They can host more than one RE ion, which has made it possible to use co-doping strategies like $Sm^{3+}/Dy^{3+}$ to produce white light that can be adjusted to different levels (Boudchicha et al., 2023). This means that borate glasses are a great material for studying how light is enhanced by electrons and for other advanced optical applications.

Although glasses doped with rare elements have some great features, they are associated with limitation. This is because of the naturally low level of absorption of 4f-4f transitions, which is not approved by the spin selection rules (Abdullahi et al., 2024). A good option is to add metal nanoparticles (MNPs), especially gold (Au) and silver (Ag), which show localised surface plasmon resonance (LSPR). LSPR happens when the conduction electrons in the nanoparticles move together in response to light, creating strong local electromagnetic fields. These fields increase the excitation and emission of nearby luminescent ions (Saad et al., 2017). The efficiency of the plasmonic enhancement depends on how the resonance condition between the nanoparticle LSPR band and the absorption or emission bands of the RE ions matches. Ag nanoparticles are very effective because of their strong plasmon resonance in the visible region. Au nanoparticles, on the other hand, provide broader and more thermally stable plasmonic effects. Studies have shown these effects: Glasses that contain the substance $Sm^{3+}$ and boron, and which also have silver particles in them, showed much brighter orange-red colour and were much more efficient, $Dy^{3+}$-doped borate glasses that also contain Au or Ag nanoparticles showed a yellow colour that was 1.1 to 2.2 times brighter than the samples without nanoparticles (Ahmad et al., 2020). Moreover, it was established that plasmonic nanoparticles also influences the colour display. They can adjust the colour temperature and tint of the light, allowing them to create a custom white light for solid-state lighting. Despite these positive results, most reports focus on singly doped RE glasses or systems with only one type of nanoparticle. The combined effects of two types of Au/Ag nanoparticles in $Sm^{3+}/Dy^{3+}$ codoped borate glasses have yet to be fully explored.

To understand and predict how rare-earth-doped glasses behave optically, we need a way to connect the experimental absorption spectra to the intrinsic radiative properties. The Judd–Ofelt (JO) theory, which was introduced separately by Judd and Ofelt, is still the most commonly used way to analyses this. The theory provides three intensity parameters ($\Omega_2$, $\Omega_4$, $\Omega_6$) which describe the local environment of RE ions in a glass host. These parameters show how for example, the symmetry, covalency and rigidity of the coordination environment are affected by changes in the glass composition (Tafida et al., 2023). How likely is it that a transition will happen and how strong the

DOI: https://doi.org/10.57233/ijsgs.v11i3.949 ISSNp: 2488-9229; ISSNe: 3027-1118



emitted light is can be predicted using the JO theory via the intensity parameters. Hence, JO analysis is a very important tool for designing efficient and reliable optical materials (Boudchicha et al., 2023). For example, JO analysis has shown that, in $Dy^{3+}$-doped borate glasses, the $^4F_{9/2} \rightarrow {}^6H_{13/2}$ yellow colour transition is the most common, which confirms that it is important for generating white light (Ahmad et al., 2020). JO analysis of $Sm^{3+}$-doped borate glasses also showed a link between $\Omega_2$ values and the degree of site asymmetry. This had a direct effect on emission intensities. Studies have recently added to the JO theory. This was done using codoped systems, such as glasses that contain $Sm^{3+}$ and $Dy^{3+}$. These studies showed that the JO theory works well for analysing how energy moves around. Despite these advances, no systematic JO analysis has yet been applied to $Sm^{3+}/Dy^{3+}$ codoped borate glasses co-embedded with dual plasmonic nanoparticles. This means that the combined effects of codoping and LSPR on radiative parameters have not yet been investigated.

The aim of this study is to reveal the effects of silver and gold nanoparticle co-embedment on the effect of JO intensity parameters in the present glass host. This will indeed pave a way for the understanding of the dynamics of the associated luminescence and allow for advanced scientific and technological applications.

## 2.0 MATERIALS AND METHOD

Melt-quenching technique was used to synthesized a series of glasses comprising of $68B_2O_3$- $15BaSO_4$-$15TeO_2$-$1Sm_2O_3$-$1Dy_2O_3$-0.1AuNps-xAgNps mol% (x = 0.03, 0.1, 0.3, and 0.7 mol%, respectively) with the powdered AgNps introduced into the host in excess. Sigma Aldrich chemicals with 99.9% purity were used for the glass synthesis, the details can be obtained from our earlier work (Abdullahi, Hashim, Ghoshal, & Sa'ad, 2020). Moreover, 99.9% purity AgNps in powder form was introduced into the glass as the co-embedder. The mixture was heated at 1300 $^oC$ for one hour and then annealed at 400 $^oC$ before being gradually cooled to room temperature. The details of the composition of the individual glasses and their codes was presented in Table 1. XRD profile detection was done using Rigaku BD68000165-01 X-ray Diffractometer (2θ range of 20 to 100$^o$) while UV–Vis-NIR absorption measurement was done usinga Shimadzu 3600Plus spectrometer (300 to 1800 nm). Furthermore, photoluminescence (PL) emission traits were recorded using Fluoromax-4C spectrophotometer adopting 402 nm excitation in the wavelength range of 300 to 750 nm. Finally, the glass densities were determined by employing Archimedes principle with Toluene as the immersion liquid.

**Table 1. Glass Compositions and the Glass Codes**

| Glass Code | Glass Composition (mol%) |
|---|---|
| S0 | $(B_2O_3)_{0.68}$- $(BaSO_4)_{0.15}$-$(TeO_2)_{0.15}$-$(Sm_2O_3)_{0.1}$-$(Dy_2O_3)_{0.1}$-$(AuNps)_{0.001}$-$(AgNps)_{0.0}$ |
| S1 | $(B_2O_3)_{0.68}$- $(BaSO_4)_{0.15}$-$(TeO_2)_{0.15}$-$(Sm_2O_3)_{0.1}$-$(Dy_2O_3)_{0.1}$-$(AuNps)_{0.01}$-$(AgNps)_{0.003}$ |
| S2 | $(B_2O_3)_{0.68}$- $(BaSO_4)_{0.15}$-$(TeO_2)_{0.15}$-$(Sm_2O_3)_{0.1}$-$(Dy_2O_3)_{0.1}$-$(AuNps)_{0.01}$-$(AgNps)_{0.01}$ |
| S3 | $(B_2O_3)_{0.68}$- $(BaSO_4)_{0.15}$-$(TeO_2)_{0.15}$-$(Sm_2O_3)_{0.1}$-$(Dy_2O_3)_{0.1}$-$(AuNps)_{0.01}$-$(AgNps)_{0.03}$ |
| S4 | $(B_2O_3)_{0.68}$- $(BaSO_4)_{0.15}$-$(TeO_2)_{0.15}$-$(Sm_2O_3)_{0.1}$-$(Dy_2O_3)_{0.1}$-$(AuNps)_{0.01}$-$(AgNps)_{0.07}$ |

## 3.0 RESULTS AND DISCUSSION

In the Results section, summarize the collected data and the analysis performed on those data relevant to the discourse that is to follow. Report the data in sufficient detail to justify your conclusions. Mention all relevant results, including those that run counter toexpectation; be sure to include small effect sizes (or statistically nonsignificant findings) when theory predicts large (or statistically significant) ones. Do not hide uncomfortable results by omission. Do not include individual scores or raw data with the exception, for example, of single-case designs or illustrative examples. In the spirit of data sharing (encouraged by APA and other professional associations and sometimes required by funding agencies), raw data, including study characteristics and individual effect sizes used in a meta -analysis, can be made available on supplemental onlinearchives.

### 3.1 X-ray diffraction (XRD) Analysis

The XRD pattern of the base glass sample as a representation is shown in Figure 1. The shown pattern is clearly devoid of any sharp peak, thus, confirming the glassy and amorphous nature of the current hosts (Ande et al., 2021; Van Tuyen et al., 2023). Furthermore, based on the available literature, the introduction of metallic nanoparticles at low concentration into glassy hosts has no effect on the XRD pattern (Hammi & El Haimeur, 2023; Holder & Schaak, 2019; Jendrzejewska, 2020), hence the reason of presenting the XRD pattern of only the base glass.

DOI: https://doi.org/10.57233/ijsgs.v11i3.949

ISSNp: 2488-9229; ISSNe: 3027-1118

IJSGS FUGUSAU VOL.11(3)

WEBSITE: https://fugus-ijsgs.com.ng

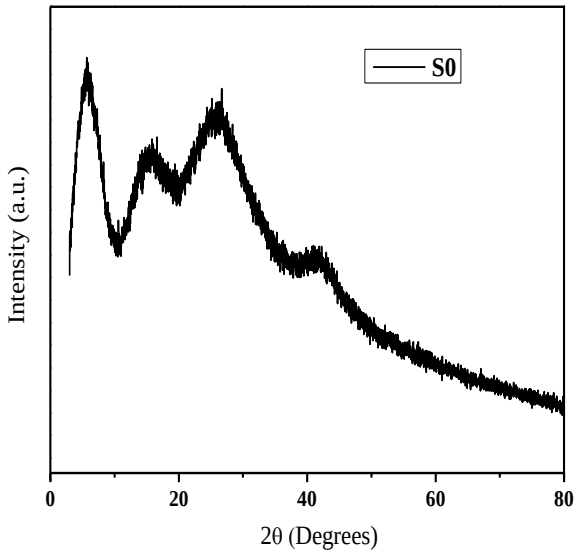


**Figure 1. XRD Pattern of S0 Glass Sample**

### 3.2 Ultraviolet-Visible-Near InfraRed optical absorption analysis

The room temperature Ultraviolet-Visible-Near Infra-Red absorption spectra for the as-synthesized samples was elucidated in Figure 2 demonstrates. The spectra was measured by setting the spectrometer at normal mode, medium scan speed, single sampling, 0.5 seconds time constant, and 1 nm wavelength interval. Out of the eleven traced, six prominent ones were selected for the JO analysis. The revealed bands coincided with the f-f transitions of both $Dy^{3+}$ and $Sm^{3+}$, similar result was obtained in literature such as (Elkhoshkhany et al., 2021; Gurav et al., 2024). Notwithstanding, the localized surface plasmon band of the co-embedded silver nanoparticles could not be visualized due to the fact that the silver atoms in the glasses are ionic in nature (Ennouri et al., 2022), it is also likely that the imbrication of the localized surface plasmon band with the $Dy^{3+}$ and $Sm^{3+}$ transitions results in the plasmon band being dominated and hence could not be seen. Moreover, from Figure 2, it could be perceived that the absorbance intensity of the glass samples varies irregularly with the concentration of silver nanoparticles, a similar trend observed by Bouabdalli et al in the case of europium doped strontium phosphate glasses (Bouabdalli et al., 2023) and Ennouri et al in the case of Ag embedded fluorophosphates glasses (Ennouri et al., 2022). While the addition of 0.03 mol% of AgNPs saw the reduction in the absorption intensity as revealed by S2 glass sample, the addition of 0.1 mol% of silver nanoparticles saw the enhancement of the absorbance attaining the highest value as proved by S3 glass sample. The most probable explanation of the observed irregular intensity variation is the imbalance between local field enhanced enjoyed by $Dy^{3+}$ and $Sm^{3+}$ at low silver nanoparticles concentration combined with absorption intensity quenching at higher silver nanoparticles concentration (Hua et al., 2018; Keshavamurthy et al., 2022; Rivera et al., 2023), another possible reason is the coupling of the gold/silver nanoparticles localized plasmon resonance which then produced varying an not proportional intensity increments. Due to the potential of optimizing absorption cross-section, the observed irregular absorption intensity may allow the production of multi-wavelength and tunable laser system useful for laser systems.

Furthermore, the overlapped $Dy^{3+}$ and $Sm^{3+}$ transition ($^6F_{11/2}$ (Dy) + $^6F_{7/2}$ (Sm)) at 1243 nm was found to be the broadest and most intense thanks to the allowed spin selection rule. While the intensity of the transitions in the visible region spanning 500 to 750 nm diminished, transitions in the ultraviolet region of 800 - 1600 nm are stronger. The diminishing of visible region transitions and the strongness of the infrared transitions is due to the forbidden spin and allowed spin selection rules, respectively (Monisha et al., 2021; Norul et al., 2022). Furthermore, the broadness of the absorption band is related to the absorption cross-section and by extension, to the gain of a laser system. Thus, the witnessed broadness could allow the laser system to be pumped with variety of sources (pumping flexibility), a crucial property needed for military warfare lasers.

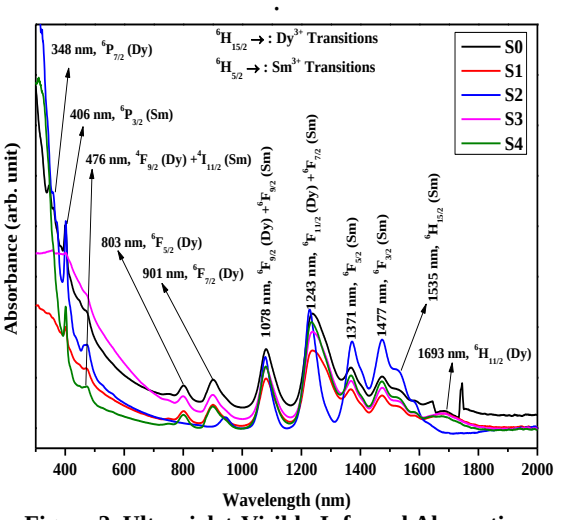


**Figure 2. Ultraviolet-Visible-Infrared Absorption Spectra of the Glass Samples**

### 3.3 Optical properties of the fabricated glass samples

It is known that the optical properties of glasses is related to electronics structure, hence, the indirect bandgap energies of the fabricated glasses were

DOI: https://doi.org/10.57233/ijsgs.v11i3.949 ISSNp: 2488-9229; ISSNe: 3027-1118



obtained from the absorption spectra using Tauc plot. Figure 3 elucidates the Tauc plot while Table 2 presents the corresponding bandgap energies along with other optical properties. Moreover, indirect bandgap energy gives more accurate predictions for glasses, especially in chalcogenide, borate, or oxide-based systems (Kumari et al., 2021) and is therefore is adopted in the current work. As clearly seen from Table 2, the introduction of the silver nanoparticles co-embedder saw the increase in the bandgap energy from 2.466 to 2.7 and then to 2.9 eV, similar observation was reported by REF. it is well documented that the refractive index of glass hosts relates to the electric dipole transition probabilities in Judd–Ofelt theory through the Lorentz local field correction. Hence, the higher the refractive index, the higher the local field symmetry of the RE ions surroundings REF. Ravindra method was used herein for the refractive index determination (Ravindra, 1981) from which other optical properties such as dielectric constant, optical dielectric constant, and reflection loss were obtained.detail of primary analyses). Consider putting the detailed results of these analyses on the supplemental online archive. Discuss the implications, if any, of the ancillary analyses for statistical error rates.

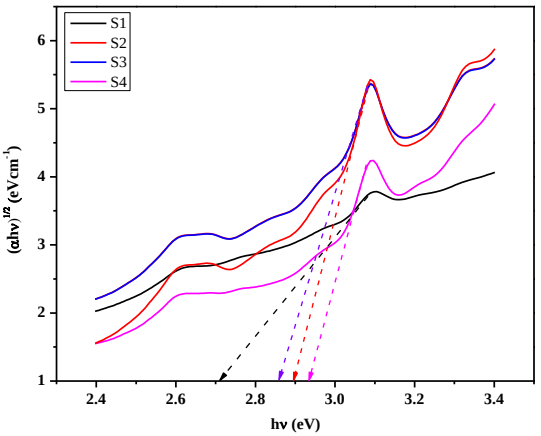


**Figure 3. Tauc's Plot for Indirect Bandgap Energy Determination**

**Table 2:** Optical Properties of the Samples

| Optical Parameter | Glass Sample | | | | |
|---|---|---|---|---|---|
| | S0 | S1 | S2 | S3 | S4 |
| Indirect Bandgap energy (eV) | 2.466 | 2.700 | 2.900 | 2.860 | 2.930 |
| Refractive index | 1.786 | 2.410 | 2.286 | 2.311 | 2.267 |
| Dielectric constant $\varepsilon$ | 3.080 | 5.808 | 5.226 | 5.341 | 5.139 |
| Optical Dielectric constant £ | 2.080 | 4.808 | 4.226 | 4.341 | 4.139 |
| Reflection loss R | 7.510 | 17.097 | 15.316 | 15.678 | 15.040 |

### 3.4 Judd-Ofelt analysis

Oscillator strength ($f$) estimates the possibility of occurrence of an optical transition between two electronic energy levels (Abdullahi, Hashim, Ghoshal, & Sa'ad, 2020). Thus, it defines the strength of ionic optical absorption/emission matching a given wavelength. Furthermore, oscillator strength being related to the integrated absorption coefficient over a transition band, is the bedrock of Judd–Ofelt analysis because it serves as the experimental input used to derive the Judd–Ofelt intensity parameters. The experimental ($f_m$) and theoretical ($f_c$) oscillator strengths associated with the current S0, S1, S2, S3, and S4 glass samples were derived using the theoretical formulations of references (Ofelt, 1962) and are presented in Table 3. Prominent $Dy^{3+}$ absorption bands were chosen for the oscillator strength determination. While the oscillator strength of transition $^6F_{5/2}$ decreased from 0.374 to 0.178 $\times 10^{-6}$ that of $^6F_{7/2}$ increased from 0.589 to 0.594$\times 10^{-6}$ with the introduction of the silver nanoparticles co-embedder. The observed trend may be associated with the change in symmetry of the RE ion surroundings.

**Table 3. Oscillator Strengths of the As-Synthesized Glass Samples**

| Transition | Oscillator Strength ($\times 10^{-6}$) | | | | | | | | | |
|---|---|---|---|---|---|---|---|---|---|---|
| | S0 | | S1 | | S2 | | S3 | | S4 | |
| | $f_m$ | $f_c$ | $f_m$ | $f_c$ | $f_m$ | $f_c$ | $f_m$ | $f_c$ | $f_m$ | $f_c$ |
| $^6F_{3/2}$ | - | - | 0.178 | 0.0008 | 0.183 | 0.022 | 0.181 | 0.0054 | 0.183 | 0.010 |
| $^6F_{5/2}$ | 0.374 | 0.285 | 0.178 | 0.00046 | 0.183 | 0.113 | 0.181 | 0.029 | 0.367 | 0.103 |
| $^6F_{7/2}$ | 0.589 | 0.663 | 0.594 | 0.045 | 0.540 | 0.498 | 0..907 | 0.510 | 0.795 | 0.746 |
| $^6F_{9/2}$ | 0.941 | 0.930 | 1.546 | 1.626 | 2.256 | 2.310 | 1.813 | 1.978 | 2.201 | 2.253 |
| $^6F_{11/2}$ | 1.955 | 1.957 | 2.973 | 2.947 | 4.389 | 4.367 | 4.956 | 4.906 | 6.113 | 6.094 |
| $^6H_{11/2}$ | - | - | 0.0594 | 0.165 | 0.05 | 0..144 | 0.212 | 0.397 | 0.611 | 0.700 |

DOI: https://doi.org/10.57233/ijsgs.v11i3.949 ISSNp: 2488-9229; ISSNe: 3027-1118

IJSGS FUGUSAU VOL.11(3) WEBSITE: https://fugus-ijsgs.com.ng

The Judd-Ofelt (JO) intensity parameters ($\Omega_2$, $\Omega_4$ and $\Omega_6$) as shown in Table 4 were derived from the presented experimental oscillator strengths. Therein, the magnitude of $\Omega_2$ corresponding to S0 decreased down to 0.81 from $1.15\times10^{-20}$ and then reduced further to $0.58\times10^{-20}$ with the insertion of silver nanoparticles co-embedder at varying content. Perhaps, structural re-adjustments within the glass network as instigated by the silver nanoparticles is responsible for the observed fluctuations.

**Table 4. Judd-Ofelt Intensity Parameters of the As-Synthesized Glass Samples**

| Glass Code | $\Omega_2$ ($\times10^{-20}$ cm$^2$) | $\Omega_4$ | $\Omega_6$ | pattern |
|---|---|---|---|---|
| S0 | 1.15 | 0.81 | 0.58 | $\Omega_2>\Omega_4>\Omega_6$ |
| S1 | 1.73 | 2.66 | -9.50 | $\Omega_4>\Omega_2>\Omega_6$ |
| S2 | 2.35 | 4.18 | -2.36 | $\Omega_4>\Omega_2>\Omega_6$ |
| S3 | 5.58 | 3.33 | -5.97 | $\Omega_2>\Omega_4>\Omega_6$ |
| S4 | 8.39 | 3.29 | 2.14 | $\Omega_2>\Omega_4>\Omega_6$ |

## 4.0 CONCLUSION

A series of new type borate based glass samples was successfully synthesized and characterized. Judd-Ofelt analysis was done and the results indicates enhanced optical absorption and emission by $Dy^{3+}$ ions due to oscillator strengths improvement which is linked to symmetry change of the ionic surroundings. The recorded enhancement was stimulated by silver nanoparticles co-embedment with gold nanoparticles. Due to the achieved striking absorption and emission cross-sections, we suggests that the present glass-REions-metallic nanoparticles combination may be useful for laser and white light emitting diodes applications.

## ACKNOWLEDGEMENTS

The authors wish to acknowledge the financial support from the Nigeria tertiary education trust fund (Tetfund) through Institution Based Research Grant (IBR) with allocation number TETF/DR&D/CE/UNIUSAU/IBR/2025/VOL.1.

## REFERENCES

Abdullahi, I., Hashim, S., & Ghoshal, S. K. (2019). Waveguide laser potency of samarium doped BaSO4-TeO2-B2O3 glasses : Evaluation of structural and optical qualities. Journal of Luminescence, 216(April), 116686. https://doi.org/https://doi.org/10.1016/j.jlumin.2019.116686

Abdullahi, I., Hashim, S., Ghoshal, S. K., & Ahmad, A. U. (2020). Structures and spectroscopic characteristics of barium-sulfur-telluro-borate glasses : Role of Sm3+ and Dy3+ Co-activation. Materials Chemistry and Physics, 247(February), 122862. https://doi.org/10.1016/j.matchemphys.2020.122862

Abdullahi, I., Hashim, S., Ghoshal, S. K., & Sa'ad, L. (2020). Modified structure and spectroscopic characteristics of Sm3+/Dy3+ co-activated barium-sulfur-telluro-borate glass host: role of plasmonic gold nanoparticles inclusion. Optics & Laser Technology, 132, 106486. https://doi.org/https://doi.org/10.1016/j.optlastec.2020.106486

Abdullahi, I., Hashim, S., Ghoshal, S. K., Sayyed, M. I., & Thabit, H. A. (2024). Significant greenish–yellow emission from Dy3+/Sm3+ co-doped strontium–aluminate–telluro-borate glasses: role of Ag and CuO nanoparticles interplay. Journal of Materials Science, 1–19. https://doi.org/10.1007/s10853-023-09276-8

Ahmad, A. U., Hashim, S., & Ghoshal, S. K. (2020). Spectroscopic characteristics of Dy3+ impurities–doped borate-based glasses: Judd–Ofelt calculation. Materials Chemistry and Physics, 253, 123386. https://doi.org/https://doi.org/10.1016/j.matchemphys.2020.123386

Ande, A., Bhemarajam, J., Kanneboina, V., Swapna, & Prasad, M. (2021). Influence of Ag nano particles on spectroscopic and luminescence properties of Dy3+ doped borate glasses. Journal of Non-Crystalline Solids, 559, 120702. https://doi.org/https://doi.org/10.1016/j.jnoncrysol.2021.120702

Basha, B., Hammoud, A., Nikolaev, A. A., Vasileva, L. V, Galutskiy, V. V, & Al-Buriahi, M. S. (2024). Terbium(III) oxide as rare earth metal modifier in PbO/Bi2O3 sodium borate glasses for highly efficient optoelectronic devices: Synthesis, characterization, and applications. Ceramics International, 50(12), 21638–21644. https://doi.org/https://doi.org/10.1016/j.ceramint.2024.03.276

Bouabdalli, E. M., El Jouad, M., Gaumer, N., Siniti, M., Touhtouh, S., & Hajjaji, A. (2023). Structural, physical, thermal and optical spectroscopy studies of the europium doped strontium phosphate glasses. Inorganic Chemistry Communications, 151(September 2022), 110563. https://doi.org/10.1016/j.inoche.2023.110563

Boudchicha, N., Iezid, M., Goumeidane, F., Legouera, M., Prasad, P. S., & Rao, P. V. (2023). Judd–Ofelt Analysis and Spectroscopy Study of Tellurite Glasses Doped with Rare-Earth (Nd3+, Sm3+, Dy3+, and Er3+). Materials, 16(21). https://doi.org/10.3390/ma16216832

Elkhoshkhany, N., Marzouk, S., El–Sherbiny, M., Anwer, H., Alqahtani, M. S., Algarni, H., Reben, M., & Sayed Yousef, E. (2021). Investigation of structural and luminescence properties of borosilicate glass doped with Dy2O3. Results in Physics, 27, 104544. https://doi.org/https://doi.org/10.1016/j.rinp.2021.104544

Ennouri, M., Petit, L., & Elhouichet, H. (2022). Investigations of the thermal, structural, and Near-IR emission properties of Ag containing fluorophosphate glasses and their crystallization process. Optical Materials, 131(May), 112610. https://doi.org/10.1016/j.optmat.2022.112610

Ghosh, S., Jana, S., & Biswas, J. (2022). Structural, thermal and spectroscopic properties of samarium (Sm3+) doped tungsten zinc tellurite glass for application in orange light emitting devices. Physica B: Condensed Matter, 644, 414205.

Gurav, B., Devidas, G. B., Dinkar, A., Surzhikova, D. P., & Rajaramakrishna, R. (2024). Instigating the Asymmetry of Dy3+ Ions Doped in Borate Glasses for Photonic Device w-LED Applications. Journal of Optics and Photonics Research, 00(March 2024), 1–11. https://doi.org/10.47852/bonviewjopr42022256

Hammi, M., & El Haimeur, A. (2023). Structural and morphological characterizations of glass based composites in thin films form. Heliyon, 9(4), e14967. https://doi.org/10.1016/j.heliyon.2023.e14967

Holder, C. F., & Schaak, R. E. (2019). Tutorial on Powder X-ray Diffraction for Characterizing Nanoscale Materials. ACS Nano, 13(7), 7359–7365. https://doi.org/10.1021/acsnano.9b05157

Hossain, M. K., Raihan, G. A., Akbar, M. A., Kabir Rubel, M. H., Ahmed, M. H., Khan, M. I., Hossain, S., Sen, S. K., Jalal, M. I. E., & El-Denglawey, A. (2022). Current Applications and Future Potential of Rare Earth Oxides in Sustainable Nuclear, Radiation, and Energy Devices: A Review. ACS Applied Electronic Materials, 4(7), 3327–3353. https://doi.org/10.1021/acsaelm.2c00069

Hua, C., Shen, L., Pun, E. Y. B., Li, D., & Lin, H. (2018). Dy3+ doped tellurite glasses containing silver nanoparticles for lighting devices. Optical Materials, 78, 72–81. https://doi.org/https://doi.org/10.1016/j.optmat.2018.02.006

Jendrzejewska, I. (2020). Application of X-Ray Powder Diffraction for Analysis of Selected Dietary Supplements Containing Magnesium and Calcium. Frontiers in Chemistry, 8(September), 1–12. https://doi.org/10.3389/fchem.2020.00672

Keshavamurthy, K., Gurushantha, K., Sayyed, M. I., Almousa, N., Mahaboob Pasha, U., Jagannath, G., & Ramesh, P. (2022). Silver nanoparticles improved infrared photoluminescence of Nd3+ doped sodium borate glasses. Infrared Physics & Technology, 127, 104451. https://doi.org/https://doi.org/10.1016/j.infrared.2022.104451

Kumari, C., Sharma, P., & Katyal, S. (2021). Different Models For Calculating The Refractive Index And Band Gap For Chalcogenide Glasses.

Li, J., Liu, J., Ni, Q., Zhu, Q., Zeng, Z., Huo, J., Long, C., & Wang, Q. (2022). Key Role Effect of Samarium in Realizing Zero Thermal Quenching and Achieving a Moisture-Resistant Reddish-Orange Emission in Ba3LaNb3O12:Sm3+. Inorganic Chemistry, 61(44), 17883–17892. https://doi.org/10.1021/acs.inorgchem.2c03231

M.C., I., Aliyu, A., S.G., M., Sabo, M., Mikailu, A., Ismaila, A., Abdullahi, I., & S.S., M. (2012). Mastering the Basics of Physics. Ahmadu Bello University Press.

Monisha, M., Murari, M. S., Sayyed, M. I., Al-Ghamdi, H., Almuqrin, A. H., Lakshminarayana, G., & Kamath, S. D. (2021). Thermal, structural and optical behaviour of Eu3+ ions in Zinc Alumino Boro-Silicate glasses for bright red emissions. Materials Chemistry and Physics, 270, 124787. https://doi.org/10.1016/J.MATCHEMPHYS.2021.124787

Muhammad, S. B., Abdullahi, I., Muhammad, H. I., & Usmman, Y. (2022). LIGAND FIELD PARAMETERS OF SAMARIUM ACTIVATED ALUMINO-BORATE BASED GLASSES. Journal of Applied Physics, 90(5), 8061–8067. https://doi.org/10.1007/s10812-023-01640-5

Norul, S., Zalamin, F., Hafiz, M., Zaid, M., Amin, K., Khalis, M., Karim, A., Afiqah, N., Yamin, M., Atikah, N., & Ismail, N. (2022). Comprehensive study on optical and luminescence properties of Sm3+ doped magnesium borotellurite glasses. Journal of Physics and Chemistry of Solids, 163(October 2021), 110563. https://doi.org/10.1016/j.jpcs.2021.110563

Ofelt, G. S. (1962). Intensities of Crystal Spectra of Rare-Earth Ions. The Journal of Chemical Physics, 37(3), 511–520. https://doi.org/10.1063/1.1701366

Phi, V., Xuan, V., Do, P. Van, Duy, L., & Xuan, N. (2019). An in-depth study of the Judd-Ofelt analysis , spectroscopic properties and energy transfer of Dy3+ in alumino-lithium-telluroborate glasses. Journal of Luminescence, 210(November 2018),

435–443. https://doi.org/10.1016/j.jlumin.2019.03.009

Ravindra, N. M. (1981). Energy gap-refractive index relation - some observations. Infrared Physics, 21(5), 283–285. https://doi.org/10.1016/0020-0891(81)90033-6

Rivera, A., Lazcano, Z., González, A. L., & Meza, O. (2023). Plasmon-enhanced luminescence of rare-earth ions by gold and silver nanoparticles in PMMA. Materials Today Communications, 34, 104967. https://doi.org/https://doi.org/10.1016/j.mtcomm.2022.104967

Saad, M., Stambouli, W., Mohamed, S. A., & Elhouichet, H. (2017). Ag nanoparticles induced luminescence enhancement of Eu3+ doped phosphate glasses. Journal of Alloys and Compounds, 705, 550–558. https://doi.org/https://doi.org/10.1016/j.jallcom.2016.12.410

Singh, S., Singh, D., Siwach, P., Gupta, I., & Kumar, P. (2025). Synthesis Strategies for Rare Earth Activated Inorganic Phosphors: A Mini Review. Applied Research, 4(1), e202400190. https://doi.org/https://doi.org/10.1002/appl.202400190

Tafida, R. A., Thakur, S., Onimisi, M. Y., Adamu, S. B., & Lakin, I. I. (2023). Samarium nanoparticle-doped silver oxide-incorporated zinc tellurite glass system: Structural, elastic, and Judd-Offelt intensity parameters. Materials Chemistry and Physics, 296, 127319. https://doi.org/https://doi.org/10.1016/j.matchemphys.2023.127319

Van Tuyen, H., Hong, T. T., Van Thanh Son, L., Lien, N. T. Q., Doddoji, R., Nguyen, H. B., & Son, L. V. T. (2023). Effects of Ce3+/Sm3+ co-doping as a luminescent modifier in borotellurite glasses for solid-state lighting. Journal of Materials Science: Materials in Electronics, 34(10), 896. https://doi.org/10.1007/s10854-023-10265-5

Zhang, J., Lang, R., Zhang, X., Xu, W., & Qi, X. (2023). Impact of non-bridging oxygens on the thermal, electrical and optical properties of germanate glasses and exploration of the germanate anomaly. Ceramics International.

DOI: https://doi.org/10.57233/ijsgs.v11i3.949 ISSNp: 2488-9229; ISSNe: 3027-1118